Colloids and Surfaces B: Biointerfaces 241 (2024) 114051

Contents lists available at ScienceDirect

Colloids and Surfaces B: Biointerfaces

journal homepage: www.elsevier.com/locate/colsurfb

Controlled assembly of superparamagnetic iron oxide nanoparticle into nanoliposome for Pickering emulsion preparation

Chin Siew Sia [a,b], Beng Ti Tey [a], Bey-Hing Goh [c,d,e], Liang Ee Low [a,b,f,*]

[a] Department of Chemical Engineering, School of Engineering, Monash University Malaysia, Subang Jaya, Selangor, 47500, Malaysia
[b] Medical Engineering and Technology (MET) Hub, School of Engineering, Monash University Malaysia, Subang Jaya, Selangor, 47500, Malaysia
[c] Sunway Biofunctional Molecules Discovery Centre (SBMDC), School of Medical and Life Sciences, Sunway University, Subang Jaya, Selangor, 47500, Malaysia
[d] Faculty of Health, Australian Research Centre in Complementary and Integrative Medicine, University of Technology Sydney, Ultimo 2007, NSW, Australia
[e] Biofunctional Molecule Exploratory Research (BMEX) Group, School of Pharmacy, Monash University Malaysia, 47500 Bandar Sunway, Selangor Darul Ehsan, Malaysia
[f] Monash-Industry Plant Oils Research Laboratory (MIPO), Monash University Malaysia, Subang Jaya, Selangor, 47500, Malaysia

ARTICLE INFO

Keywords:
Superparamagnetic iron oxide nanoparticle
Magnetoliposome
Pickering emulsion
Magnetic-responsive
PH-responsive

ABSTRACT

There has been a surge in effort in the development of various solid nanoparticles as Pickering emulsion stabilizers in the past decades. Regardless, the exploration of stabilizers that simultaneously stabilize and deliver bioactive has been limited. For this, liposomes with amphiphilic nature have been introduced as Pickering emulsion stabilizers but these nano-sized vesicles lack targeting specificity. Therefore in this study, superparamagnetic iron oxide nanoparticles (SPION) encapsulated within liposomes (MLP) were used as Pickering emulsion stabilizers to prepare pH and magnetic-responsive Pickering emulsions. A stable MLP-stabilized Pickering emulsion formulation was established by varying the MLP pH, concentration, and oil loading during the emulsification process. The primary stabilization mechanism of the emulsion under pH variation was identified to be largely associated with the MLP phosphate group deprotonation. When subjected to sequential pH adjustment to imitate the gastrointestinal digestion pH environment, a recovery in Pickering emulsion integrity was observed as the pH changes from acidic to alkaline. By incorporating SPION, the Pickering emulsion can be guided to the targeted site under the influence of a magnetic field without compromising emulsion stability. Overall, the results demonstrated the potential of MLP-stabilized Pickering emulsion as a dual pH- and magnetic-responsive drug delivery carrier with the ability to co-encapsulate hydrophobic and hydrophilic bioactive.

1. Introduction

Emulsions are described as a colloidal dispersion of two or more immiscible phases in a single system [1,2]. Given the immiscibility, emulsions are thermodynamically unstable in the absence of an emulsifier. Surfactants are traditionally utilized to delay the emulsion destabilization by lowering the surface tension between the two phases. However, the use of surfactant remains controversial as it has allergenic potential and might pose environmental concerns [3,4]. On account of heightened consumer awareness and the implementation of more rigorous environmental regulations, the use of solid particles as emulsifiers to form Pickering emulsion has been introduced. Pickering emulsion have emerged as frontrunners for targeted drug delivery as they possess characteristics including enhanced stability, excellent payload capacity, and versatility *via* design engineering. A myriad of solid particles such as chitosan [5,6], cellulose nanocrystal [7,8], iron oxide nanoparticles, or the combination of these [9,10] have been utilized as Pickering emulsifiers. Despite the leap in Pickering emulsifier development, limited effort has been invested in the exploration of emulsifiers that not only stabilize but simultaneously deliver other bioactive to further augment emulsion functionality.

Liposomes are spherical nano-sized vesicles conventionally made up of amphipathic lipids that self-assemble into a bilayer structure enveloping an aqueous lumen when dispersed in water [11]. Owing to their amphiphilic nature, the encapsulation of both hydrophobic and hydrophilic drugs in the bilayer or the aqueous lumen respectively is possible, thereby broadening their application in the biomedical domain [11,12]. For the past decades, Food and Drug Administration (FDA) approved liposome formulations (Doxorubicin (Dox), Doxil, and Myocet) have been widely used in clinical settings owing to their low toxicity, and

* Corresponding author at: Department of Chemical Engineering, School of Engineering, Monash University Malaysia, Subang Jaya, Selangor, 47500, Malaysia.
E-mail address: low.liangee@monash.edu (L.E. Low).

https://doi.org/10.1016/j.colsurfb.2024.114051
Received 13 March 2024; Received in revised form 22 April 2024; Accepted 19 June 2024
Available online 21 June 2024

improved drug loading capacity [13,14]. Among different liposomal formulations, pH-responsive liposome synthesized *via* natural phospholipid (*e.g.,* phosphatidylcholine, phosphoethanolamine, *etc.*) has been largely explored [15,16]. When these liposome formulations are exposed to acidic conditions, the permeability of the membrane is affected *via* functional group protonation/deprotonation. Eventually, the bilayer membrane ruptures to trigger site-targeted cargo release. This is especially beneficial for tumor-targeted delivery as the tumor microenvironment is often more acidic than healthy tissues [17]. Other than the widespread use of stimuli-responsive liposomes as drug delivery vehicles in the biomedical field, liposomes have recently been proposed as Pickering emulsifiers to form oil-in-water Pickering emulsions [18,19]. These studies analyzed the structural stability of liposome-stabilized Pickering emulsion prepared *via* low-energy mixing to prevent compromising liposome structural integrity. In addition, the potential of liposome-stabilized Pickering emulsion as a delivery vehicle co-encapsulating hydrophobic and hydrophilic drug for in vitro release was explored [18]. Although the outcomes from these studies demonstrated that liposome-stabilized Pickering emulsion can be considered as promising drug delivery candidates, they lack targeting specificity. To harness the unique ascendancies of liposome-stabilized Pickering emulsion and overcome the abovementioned limitation, the incorporation of superparamagnetic iron oxide nanoparticles (SPION) into liposome to form magnetoliposome (MLP) as a Pickering emulsifier has been proposed in this study.

Magnetic nanoparticles in particular SPION have been widely utilized in the biomedical field for tumor-targeted diagnosis or delivery [17,20,21]. SPION is made up of an iron oxide core comprising either magnetite (Fe_3O_4) or maghemite (γ-Fe_2O_3) with a core size between 10 and 20 nm [13]. Under the exposure of an external magnetic field, SPION can be magnetized up to a high saturation intensity and promptly loses its magnetism when the field is removed. This allows SPION to travel to the targeted sites with high precision *via* remote controlling [20,22,23]. Moreover, SPION-based drug delivery systems also exhibit characteristics such as biocompatibility, improved biodistribution, improved cellular uptake, and minimal toxicity [20,23]. Since bare SPION are rather hydrophobic and have poor aqueous dispersity, hydrophilic surface modifications become necessary for their subsequent biomedical application [24]. Following their hydrophilic modifications, these SPION can be encapsulated within the aqueous lumen of liposome to form MLP, and can further be used as a Pickering emulsifier with magnetic responsiveness. While several studies have developed magnetic Pickering emulsions for the targeted delivery of hydrophobic bioactive, little attention has been given to the development of magnetic Pickering emulsions that are capable of delivering both hydrophobic and hydrophilic bioactive [25,26].

Herein, we report the preparation of Pickering emulsion by using MLP as an emulsifier that demonstrates both pH and magnetic responsiveness. The effect of MLP pH, MLP concentration, and oil loading on the formation of Pickering emulsion was evaluated by investigating their size, morphology, and creaming profile. In addition, their storage stability under different temperatures was also examined. The current work also studied the pH responsiveness of the MLP-stabilized Pickering emulsion by subjecting the emulsion to various pH environments. To validate the magnetic responsiveness of the emulsion after incorporation of SPION, the MLP-stabilized Pickering emulsion was subjected to an external magnetic field. The magnetic responsiveness of SPION was successfully retained after its encapsulation within MLP allowing magnetic-guided delivery. This work denotes the use of MLP as a Pickering emulsifier which displayed both pH and magnetic responsiveness to potentially enhance the precision of drug delivery.

2. Experimental methods

2.1. Materials

Iron (III) chloride hexahydrate ($FeCl_3{\cdot}6\ H_2O$, 99 %), sodium oleate (99.0 %), hexane (96.0 %), diphenyl ether, oleyl alcohol (technical grade, 85 %), oleic acid (99.0 %), 1,2-dichlorobenzene (99.0 %), N,N'-dimethylformamide (99.8 %), citric acid (99.0 %), diethyl ether (99.0 %). L-α-phosphatidylcholine (from soybean, Type II-S, 14–29 % choline basis), cholesterol (99.0 %), chloroform (99.0 %), and polyethylene glycol 3000 (PEG) were all purchased from Merck, Malaysia. Acetone (99.0 %), isopropyl alcohol (99.0 %), and diethyl ether (99.0 %) were purchased from Systerm Chemicals. Sunflower oil was purchased from Naturel Premium Blend, Lam Soon. Ultrapure water with a Milli-Q® Plus apparatus and resistivity of 18.2 MΩ cm^{-1} was used throughout this study (Millipore, Billerica, USA). All chemicals used in this study were of analytical grade.

2.2. Preparation of SPION

The SPION was synthesized *via* the thermal decomposition route and modified with hydrophilic moieties. Briefly, 0.1 g of sodium oleate was dissolved in 42 mL of hexane at room temperature. 0.36 g of iron (III) chloride was dissolved in 25 mL of water and 33 mL of ethanol at room temperature. The two mixtures was mixed and heated for 1 h. After 1 hour, the aqueous phase was removed and the washed mixture was dried for 24 h to obtain iron precursor. The prepared iron precursor was rapidly injected into a solution of 30 mL diphenyl ether, oleic acid, and oleyl alcohol at 100 °C under constant nitrogen purging. The mixture was heated to reflux and kept at that temperature for 1 h. During this process, the initial orange solution turns black. The resulting black solution was then cooled to room temperature and acetone was added to yield a black precipitate. The precipitate was separated by centrifugation, washed, and dried in a vacuum oven to obtain a black magnetic powder. The resulting powder was stored by redispersing it in chloroform for future analysis. To further functionalize the SPION with a hydrophilic group, 0.1 g of as-synthesized SPION was dissolved in a 1:1 mixture of 1,2-dichlorobenzene and N,N'-dimethylformamide (30 mL total volume). 1.24 g of citric acid was added and the mixture was stirred at 60 °C for 24 hours. After cooling the solution, diethyl ether was added to yield a brown precipitate. The precipitate was separated by centrifugation, washed with acetone, and dried in a vacuum oven to obtain hydrophilic citric acid-capped SPION.

2.3. Preparation of MLP

MLP was prepared by thin film hydration method. L-α-phosphatidylcholine and cholesterol at the ratio of 6:1 (total lipids 200 mg) dissolved in 10 mL of chloroform were added to a round bottom flask. Chloroform was removed using a rotary evaporator (Rotavapor® R-100, BUCHI) at 460 mbar for at least 1 h to form a thin dried lipid film. The film was then hydrated in ultrapure water containing SPION for 1 h. Unencapsulated SPION was removed by centrifuging the samples at 1000 XG for 10 min. The hydrated liposomes were extruded with 11 passages through a 220 nm pore diameter polycarbonate membrane filter using a mini extruder (Avanti Polar Lipids Inc., Alabaster, AL) to obtain uniform size distribution.

2.4. Characterization of SPION and MLP

Physicochemical analysis. The magnetization of SPION was measured using the vibrating sample magnetometry (VSM) (Lakeshore 7400 Series). The encapsulation of SPION in MLP and the mean hydrodynamic diameter of SPION and MLP were visualized using transmission electron microscopy (TEM) (TECNAI G2 F20) operating at 200 kV accelerating voltage. The zeta potential of the MLP suspension under different pH

was determined with Zetasizer Nano ZS 90 (Malvern Instruments, UK), at 25 °C.

Particle wettability analysis. The wettability of MLP was characterized based on the air-liquid contact angle measurement using the contact angle goniometer (Ramé-Hart Instrument Co., USA). Briefly, the MLP suspension was deposited on a glass slide and air-dried overnight. Eight droplets of ultrapure water were deposited on different locations of the dried film where the contact angles were then calculated.

2.5. Preparation of MLP-stabilized Pickering emulsion

Coarse emulsion formation. The oil phase was first prepared by dissolving l-α-phosphatidylcholine (emulsifier) in 10 mL chloroform. Chloroform was then removed using a rotary evaporator at 460 mbar for at least 1 h. The thin lipid film was then rehydrated using sunflower oil under magnetic stirring for 2 h to achieve a final lipid concentration of 0.25 % w/v. Preparation of the water phase included dissolving PEG in ultrapure water. PEG solution was then added to the sunflower oil and ultrasonicated for 3 min in an ice bath. The total volume of emulsion formed was 20 mL. The coarse emulsion was sent for freeze-drying at −90°C for at least 8 h.

Pickering emulsion formation. The freeze-dried emulsion was then rehydrated with MLP suspension to the initial volume for 1 h and homogenized at 10,000 RPM for 3 min to obtain MLP-stabilized Pickering emulsion.

2.6. Characterization of MLP-stabilized Pickering emulsion

Microstructural analysis. The microstructure of freshly prepared MLP-stabilized Pickering emulsion was visualized using an inverted optical microscope (Nikon Eclipse Ti-E, Nikon Instruments Inc., USA) at 20× magnification. The visualized samples were diluted 100 times, dropped on cleaned microscope slides, and observed at 20 x magnification. The fluorescent images were performed by staining the MLP with fluorescein isothiocyanate (FITC) (0.1 %v/v) prior to the Pickering emulsion formation.

Emulsion type. The type of emulsion formed in this study was verified to be either oil-in-water or water-in-oil by utilizing the drop test method where photographs were taken. Separately, the Pickering emulsion freshly formed was dropped into pure water and pure oil. From visual observation, the Pickering emulsion is categorized as an oil-in-water Pickering emulsion if well dispersed in the water phase and not the oil phase. On the contrary, if the emulsion was well dispersed in the oil phase and not the water phase, emulsion is categorized as water-in-oil Pickering emulsion.

Emulsion stability. The stability of MLP-stabilized Pickering emulsion was evaluated by visual observation of the Pickering emulsion. Upon formation, the emulsions were transferred into capped glass vials at room temperature and left undisturbed for up to 14 days. The creaming stability of the Pickering emulsion was determined by measuring the height of the stable emulsion fraction after preparation using the equation below:

$$\text{Stable emulsion, } \% = \frac{\text{Height of stable emulsion}}{\text{Total emulsion height}} \times 100\% \quad (1)$$

Physicochemical analysis. The hydrodynamic diameter and size distribution of Pickering emulsion formed for up to 14 days was measured periodically using a Mastersizer (Mastersizer 3000, Malvern Instrument, UK) equipped with a Hydro EV dispersion unit. The zeta potential of the Pickering emulsion was determined with Zetasizer Nano ZS 90 (Malvern Instruments, UK), at 25 °C.

2.7. Physicochemical Stability of MLP-stabilized Pickering emulsion

Effect of MLP pH on Pickering emulsion stability. The MLP concentration and oil volume were kept constant at 10 % w/v, and 10 % v/v respectively. The pH of the MLP suspension was adjusted using either 0.1 M HCl or 0.1 M NaOH to 1.5, 3.0, 5.0, 6.0, 7.4, and 10.0 prior to using it for the formation of MLP-stabilized Pickering emulsion. The Pickering emulsion was formed as described above and then transferred to glass vials and stored at room temperature for subsequent characterization.

Effect of MLP concentration on Pickering emulsion stability. The MLP pH and oil volume were kept constant at pH 7.4, and 10 % v/v respectively. The MLP was prepared at different concentrations (10, 20, 30, and 40 % w/v) by dissolving l-α-phosphatidylcholine and cholesterol at the ratio of 6:1 in chloroform. A thin film was formed after subjecting the mixture to rotary evaporation and subsequently rehydrated with ultrapure water containing SPION before the preparation of MLP-stabilized Pickering emulsion. The Pickering emulsion was formed as described above and then transferred to glass vials and stored at room temperature for subsequent characterization.

Effect of oil volume on Pickering emulsion stability. The MLP pH and MLP concentration were kept constant at pH 7.4, and 30 % w/v respectively. Emulsions with different oil volume fractions were prepared by homogenizing PEG with different oil volume fractions (10, 20, 30, and 40 % v/v) to achieve a final emulsion volume of 20 mL. The Pickering emulsion was formed as described above and then transferred to glass vials and stored at room temperature for subsequent characterization.

2.8. Storage stability of MLP-stabilized Pickering emulsion

The freshly prepared MLP-stabilized Pickering emulsion was then into a screw cap glass vial and stored under different temperatures (4, 25, and 45°C) for 21 days. The creaming stability and hydrodynamic diameter were then analyzed as described above.

2.9. pH responsiveness of MLP-stabilized Pickering emulsion

The pH-responsive properties of MLP-stabilized Pickering emulsion were investigated by adjusting the pH of the stable Pickering emulsion to pH 1.5, 3.0, 5.0, 7.4, and 8.5 using 1.0 M HCl or 1.0 M NaOH. The sequential pH response of MLP-stabilized Pickering emulsion was also investigated by adjusting the Pickering emulsion to pH 1.5, 8.5, and 7.4 continuously. The hydrodynamic diameter and morphology were analyzed after each pH variation.

2.10. Magnetic responsiveness of MLP-stabilized Pickering emulsion

The motion of the MLP-stabilized Pickering emulsion under the influence of an external magnetic field was examined by using a method described previously with slight modifications [10]. Briefly, 1.0 mL of stable Pickering emulsion was deposited into a petri dish filled with water and subjected to an external magnetic field by placing a magnet underneath. Photographs were taken on a digital camera to observe the motion of the MLP-stabilized Pickering emulsion. The demulsification investigation was conducted as described previously with slight modifications [27–30].

2.11. Statistical Analysis

Each set of experiments was independently performed at least twice, and the results were expressed as means and standard deviation. GraphPad Prism software was used for statistical analysis. Analysis of variance (ANOVA) was conducted and statistical significance was defined as $p \leq 0.05$.

3. Results and Discussion

3.1. Characterization of SPION and MLP

Characterization of SPION. The SPION was synthesized *via* thermal decomposition and subjected to ligand exchange with citric acid to yield hydrophilic SPION. The particle size and zeta potential of SPION was inspected using TEM and dynamic light scattering (DLS). The size of SPION was measured to be 8.8 ± 1.2 nm with a zeta potential of −36.7 ± 0.4 mV as a result of SPION surface stabilization via citric acid adsorption (Fig. 1**a**). Depending on steric necessity and surface curvature, citric acid could potentially adsorbed onto SPION surface by coordinating one or two of the carboxylate functional groups. Therefore, at least one free carboxyl group present is responsible for their hydrophilic characteristics thus improving their colloidal stability in aqueous medium [31]. In addition, the SPION showcased superparamagnetic characteristics and had a saturation magnetization (M_s) of 42.4 emu/g from the VSM analysis (Fig. 1**b**). Since superparamagnetic materials do not possess remanent magnetization, they can be instantaneously and strongly magnetized/demagnetized under the presence/absence of a small applied magnetic field [31,32]. Fundamentally, a higher M_s is ideal for magnetic targeting because the magnetic force (F_m) exerted on a magnetic nanoparticle in the presence of an applied magnetic field can be expressed as $F_m = \chi V(\nabla B)^2/(2\mu_0)$, where χ represents the particle's magnetic susceptibility, V signifies volume, ∇B denotes external magnetic field gradient and μ_0 denotes free space permeability [32]. Thus, the functionalized SPION with high M_s can be effectively guided to and retained at the targeted site under the influence of applied magnetic field [32,33]. By further co-encapsulating these SPION and biological molecules/drugs within liposome, this carrier can be magnetically concentrated at targeted site, facilitating subsequent cargo release. The released SPION can be potentially used for diagnosis (i.e., MRI contrast agent) or therapy (i.e., via magnetic hyperthermia effect or targeted drug delivery) [34–38].

Characterization of MLP. The citric acid-capped SPION was further encapsulated within the aqueous lumen of liposome *via* thin film hydration forming MLP. The size of MLP characterized using DLS was 176.9 ± 6.8 nm with a zeta potential of −51.8 ± 1.4 mV at pH 6.0. Inspection from the TEM photographs showcased successful encapsulation of SPION within the aqueous lumen of liposome without compromising liposome integrity (Fig. 1**c**). As mentioned previously, the wettability of Pickering emulsifiers plays a vital role in affecting emulsion stability

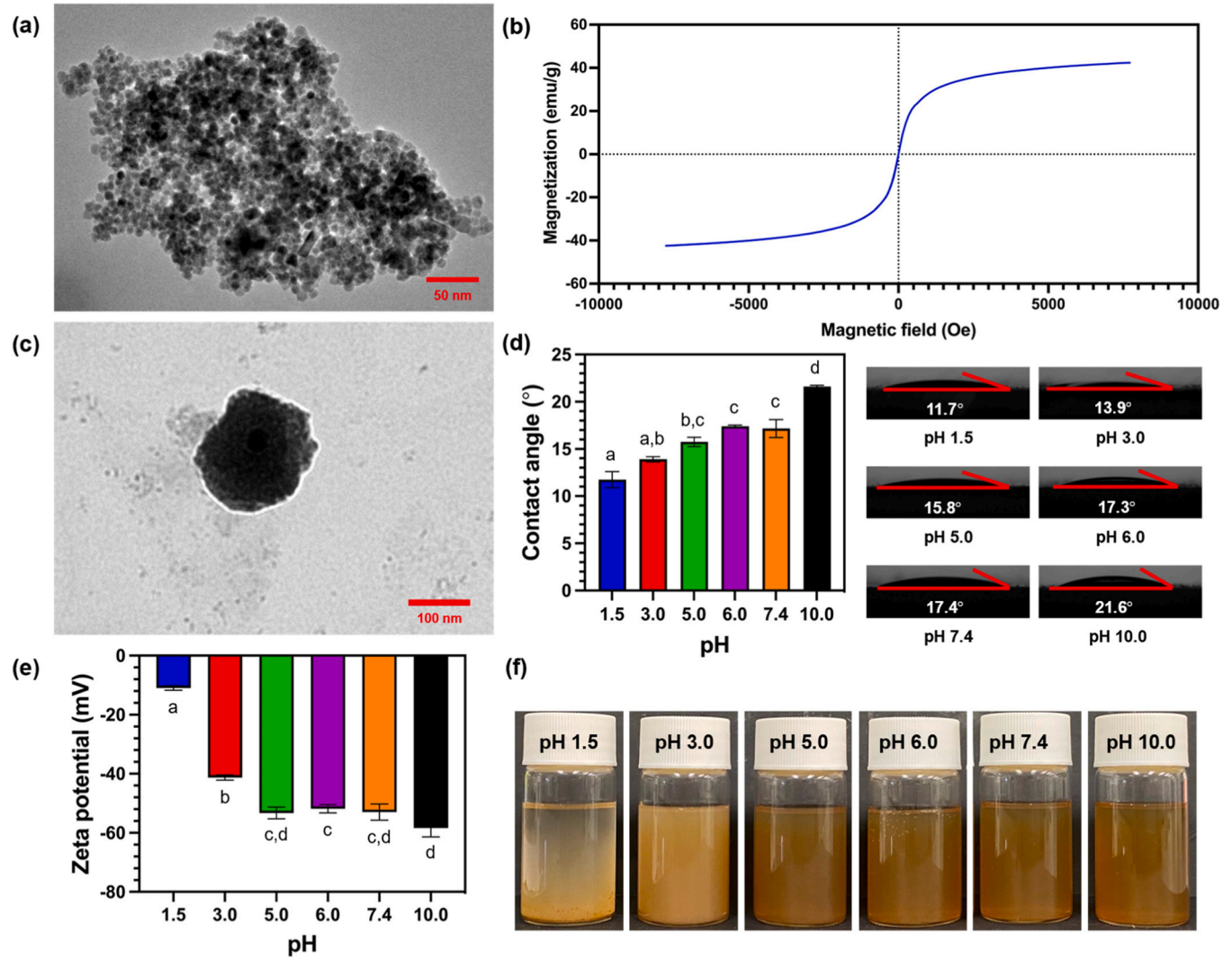

Fig. 1. Characterization of SPION. (a) HR-TEM photograph of hydrophilic SPION. (b) Magnetization curve for SPION. Characterization of MLP. (c) HR-TEM photograph of MLP. (d) Three-phase contact angle of MLP at different pH at their corresponding photographs. (e) Zeta potential of MLP at different pH. (f) Photographs of MLP at different pH. The error bars represent the standard deviation in measurements and different alphabetic letters were significantly different at $p \leq 0.05$ by Bonferroni's Multiple Comparison Test.

[39]. Given that, the wetting behavior of MLP under different pH was investigated *via* three-phase contact angle measurement. From Fig. 1**d**, the three phases contact angle exhibited a general increasing trend from $11.7 \pm 0.9^{\circ}$ to $21.6 \pm 0.1^{\circ}$ as pH increases from 1.5 to 10.0. The contact angle of MLP generally falls below 90° and thus is considered to be a hydrophilic Pickering emulsifier [39]. As discussed by Xiao, Li, and Huang, when the contact angle is within or greater than 30° but smaller than 150°, irreversible adsorption of the emulsifier will take place as the particle desorption energy is significantly larger than the thermal energy associated with Brownian motion [40]. Hence, it was expected that an enhanced emulsion stability would be reflected at a more alkaline pH.

Besides surface wettability, the magnitude of surface charges also vastly affects colloidal stability and emulsion stability. In this study, the surface charge of MLP suspension at different pH was also measured using a zetasizer. At physiological pH (pH 7.4), the MLP exhibited a surface charge of -53.0 ± 1.4 mV and its net value increased with pH (Fig. 1**e**). Whereas at a more acidic pH, the net surface charge decreased. This observation could be due to the protonation of phosphate group on phosphatidylcholine below its pK_a ($pK_{a1} = 2.2$). As pH approaches pK_a ($pK_{a2} = 7.2$ and $pK_{a3} = 12.3$), the phosphate groups further get deprotonated as corroborated by the increasingly negative surface charge (Figure S1) [41]. The protonation and deprotonation of the lipid bilayer can then disrupt the MLP structure causing bilayer membrane rupture [15]. Some might argue that the MLP disintegration could be due to chemical degradation of ester bonds, this is unlikely as ester bonds are considerably stable under acidic conditions unless exposed to specific degradative enzymes such as esterase [42,43]. It can also be observed that the MLP suspension was less turbid in a more acidic environment which could represent lipid bilayer disintegration as previously reported in other studies (Fig. 1**f**) [44]. This is unfavorable as this can cause leakage of encapsulated SPION or bioactive resulting in premature drug release. Therefore, it is of utmost importance to ensure the MLP is prepared at a pH where it can both retain its structural integrity and effectively stabilize the emulsion.

3.2. Characterization of MLP-stabilized Pickering emulsion

Although phosphatidylcholine was added in the oil phase during coarse emulsion preparation, its presence alone was insufficient to stabilize the emulsion system at low energy mixing (Figure S2). In an attempt to improve emulsion stability, MLP was added to the system. The MLP formed using the thin film hydration method was used as the emulsifier in this study. To investigate the type of emulsion formed, emulsion drop tests in pure water and pure oil were conducted. As observed, the emulsion was found to disperse well in pure water and remained as a droplet in pure oil indicating the formation of oil-in-water emulsion (Fig. 2**a**). Following that, the localization of MLP at the interface was visualized using fluorescence microscopy by staining MLP with FITC. From Fig. 2**b**, the fluorescent images revealed an evident green fluorescent ring surrounding the oil droplets demonstrating the irreversible adsorption of MLP as a Pickering emulsifier at the oil/water interface.

3.3. Factors affecting the stability of MLP-stabilized Pickering emulsion

Effect of the pH of MLP suspension. The effect of the pH of MLP suspension (1.5, 3.0, 5.0, 6.0, 7.4, and 10.0) on the formation of the Pickering emulsion was investigated by monitoring the changes in their mean droplet size and creaming profile. All Pickering emulsions were formed at PEG concentration of 5 % w/v. In the pH study, the Pickering emulsion was formed at a fixed MLP concentration and oil loading of 20 % w/v and 10 % v/v, respectively. As seen in Fig. 3**a**, the emulsion formed at pH 7.4 was relatively stable with a droplet size of 13.5 ± 0.1 μm. The size distribution curve of the emulsion formed at MLP pH > 7.4 revealed uniform size distribution indicating that the emulsion formed was monodispersed (Figure S3a). Fig. 3**b and c** showcased that although all Pickering emulsions underwent creaming, emulsions stabilized at MLP pH > 7.4 are less likely to deoil and destabilize. This can be associated with the surface charge of the MLP at different pH as liposome-

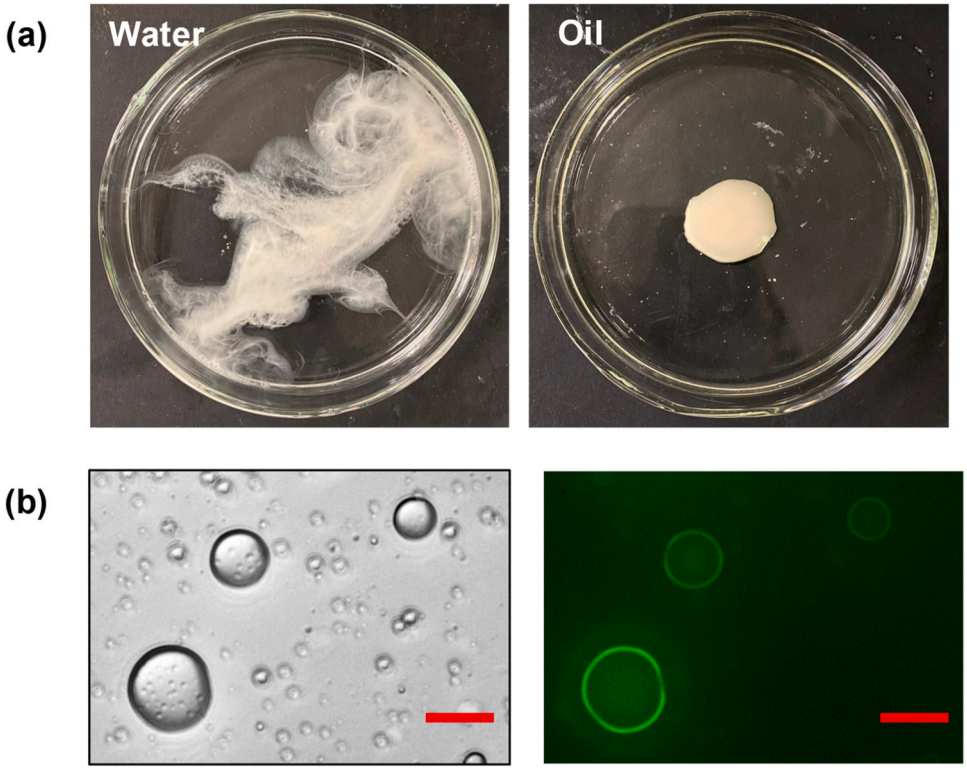

Fig. 2. Characterization of MLP-stabilized Pickering emulsion. (a) Drop test of MLP-stabilized emulsion in pure water (left) and pure oil (right). (b) Fluorescence images of Pickering emulsion showcasing the location of MLP (green fluorescence represents the location of MLP). The scale bar is 20 μm.

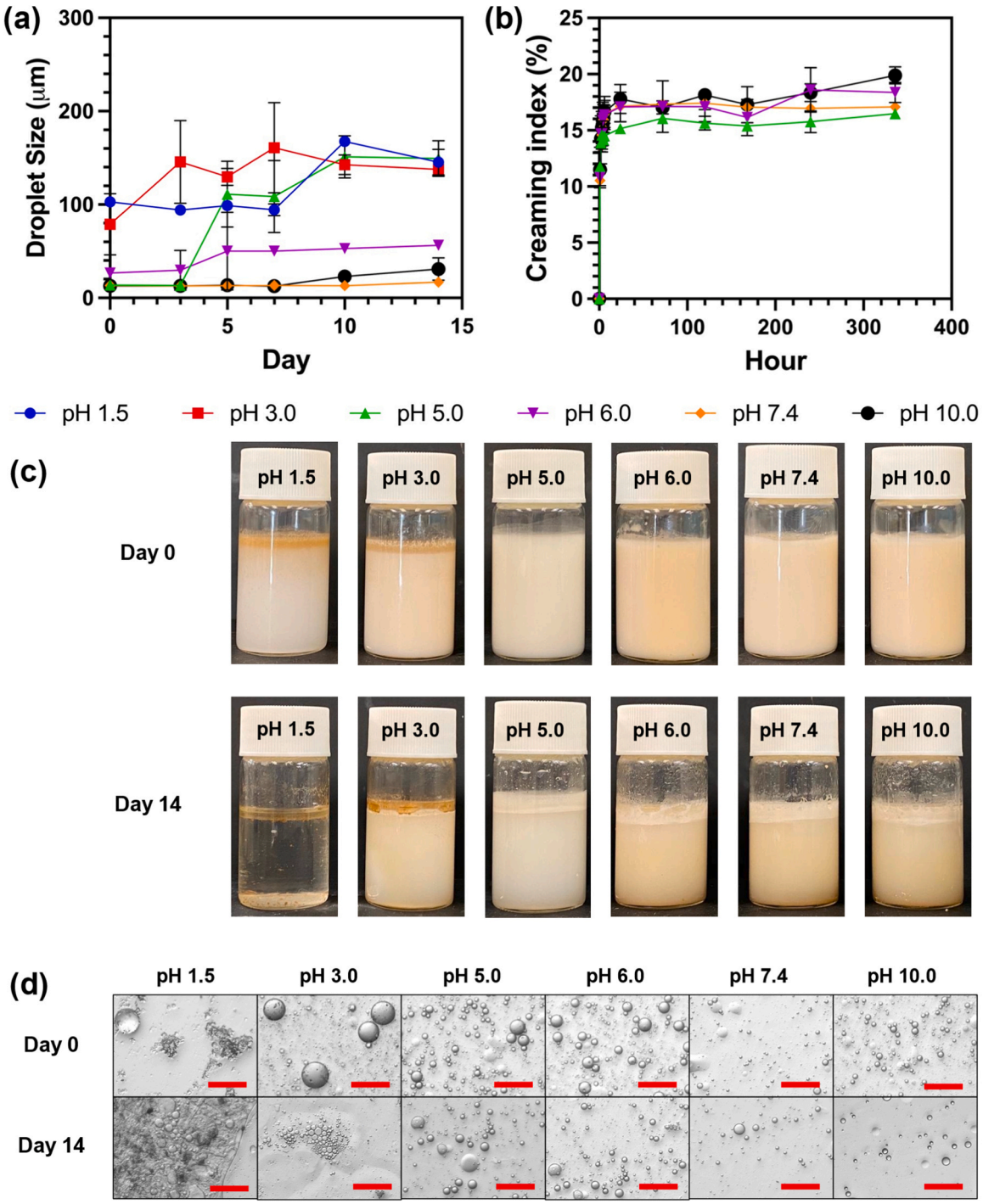

Fig. 3. Effect of MLP pH on Pickering emulsion stability. (a) Droplet size, (b) creaming index, (c) creaming profile, and (d) microscopic images of MLP-stabilized Pickering emulsion at different MLP pH from day 0 to day 14. The scale bar is 50 μm. The error bars represent the standard deviation in measurements.

stabilized Pickering emulsions are primarily stabilized by the electrostatic repulsion between individual liposome nanoparticles [19]. As pH increases, the surface charge of MLP increases negatively, and at pH > 7.4, MLP predominantly possesses negative charges. This can effectively resist particle agglomeration thus enhancing interface coverage and subsequent Pickering emulsion stability [39]. On the contrary, droplet size showcased an increasing trend under a more acidic environment. An increase in droplet size of about 10-fold was recorded as MLP pH was adjusted to pH 1.5 and 3.0 with an increasing degree of polydispersity. In addition, apparent deoiling and phase separation were observed under these conditions. At acidic pH, repulsive energy between MLP is reduced as their surface charge approaches zero. This reduction in repulsive energy consequently leads to severe particle aggregation and provides poor interface coverage, thereby prompting droplet agglomeration [45]. After storing the Pickering emulsion for 14 days, the droplet size of Pickering emulsions formed at alkali pH remained relatively stable as compared to those at acidic pH, which was in good agreement with the optical microscopic images (Fig. 3**d**).

Effect of MLP concentration. To investigate the effect of MLP concentration on Pickering emulsion stability, the MLP pH and oil volume were maintained at pH 7.4 and 10 % v/v respectively. Upon formation, all emulsion samples exhibited uniform size distribution (Figure S3b)

with similar droplet size, whereby the emulsion with the smallest droplet size (12.3 ± 0.9 μm) was obtained at 30 % w/v MLP (Fig. 4**a**). After storage for 14 days, the Pickering emulsion stabilized by 30 % w/v MLP concentration also showed the smallest size increment (from 12.3 ± 0.9 μm to 15.1 ± 1.0 μm). As a more robust oil/water interface coverage is established at higher MLP concentration, droplet coalescence is inhibited and interfacial tension is reduced. These ultimately contribute to the enhanced emulsion stability [2,19,46]. However, there was an increase in droplet size from 12.5 ± 0.9 μm to 57.4 ± 7.7 μm at 40 % w/v MLP concentration. This could be due to the presence of

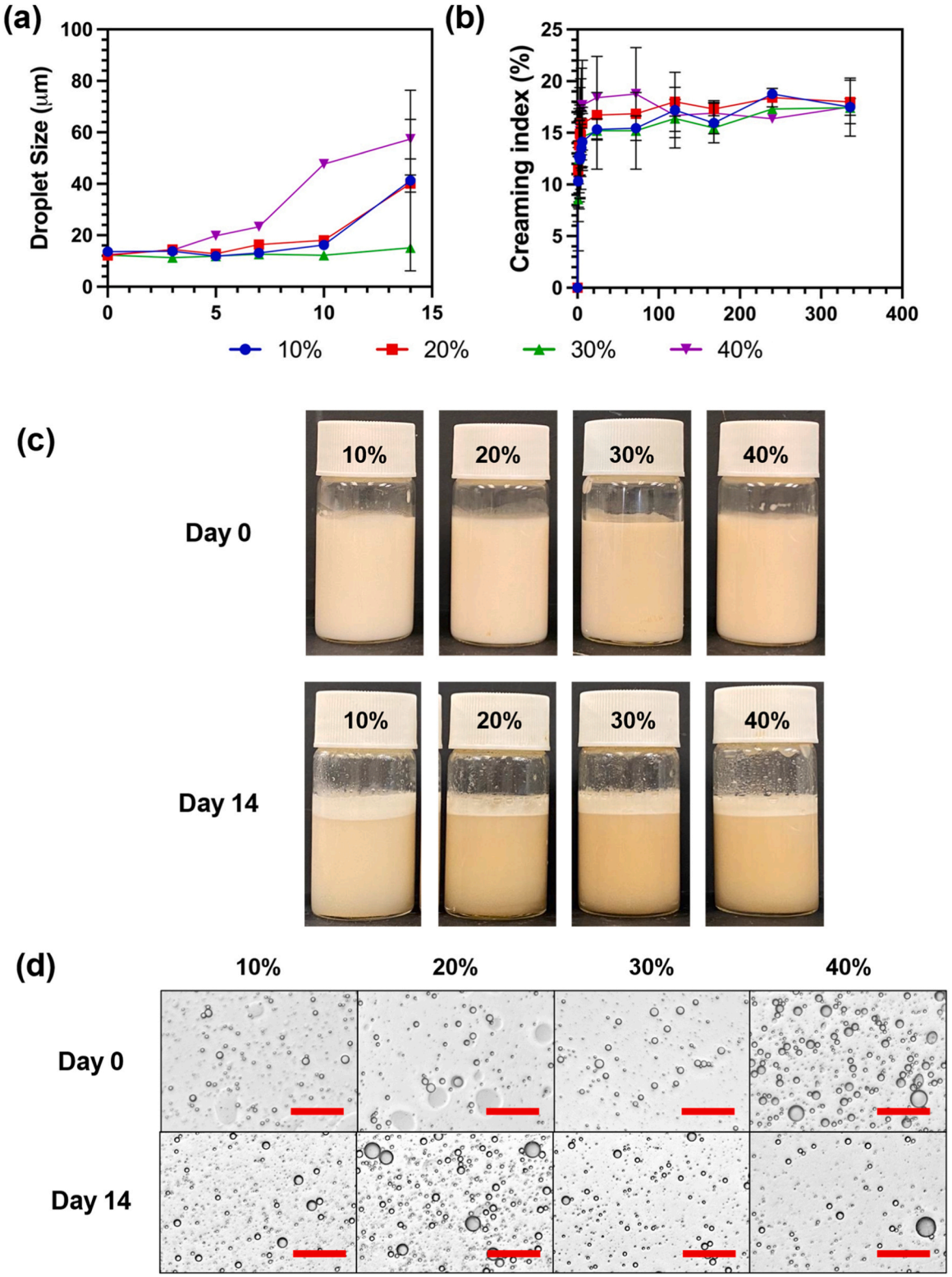

Fig. 4. Effect of MLP concentration on Pickering emulsion stability. (a) Droplet size, (b) creaming index, (c) creaming profile, and (d) microscopic images of MLP-stabilized Pickering emulsion at different MLP concentrations from day 0 to day 14. The scale bar is 50 μm. The error bars represent the standard deviation in measurements.

surplus MLP in the continuous phase in which the overcrowded MLP further led to particle aggregation and hindered particle packing at the interface [19,45]. Furthermore, the adsorption of these larger aggregated MLP at the interface contributes to an increase in the overall droplet size [19]. It can be seen from Fig. 4**b and c** that all emulsions underwent creaming. Several factors might have contributed to this, with large MLP size (~100 nm) being one of the primary factors as the size of particles can substantially affect the particle desorption energy. Generally, a smaller particle size allows for denser packing, which improves emulsion stability by reinforcing the barrier at the oil/water interface [47]. Moreover, the size of the emulsion droplet is inevitably restricted by the particle size where larger particles generally yield larger emulsion droplets [39,46]. Larger droplets accelerate the creaming process as they are more susceptible to gravitational forces as compared to the smaller ones [45]. The larger droplet sizes at 10 %, 20 %, and 40 % w/v MLP were also reflected in their microscopic images (see Fig. 4**d**).

Effect of oil volume. The effect of oil volume on the Pickering emulsion droplet size and morphology was examined at a fixed pH and MLP concentration of 7.4 and 30 % w/v respectively. By increasing the oil loading from 10 % v/v to 40 % v/v, the droplet size progressively increased from 12.3 ± 0.9 μm to 16.7 ± 0.1 μm (Fig. 5**a**). The increment was insignificant as the emulsion droplet size is limited by the MLP concentration. It was also noticed that, creaming increased with oil loading as the creaming profile is directly related to the initial oil loading volume (Fig. 5**b**). With that, creaming will eventually reach a point corresponding to the initial oil loading volume thus the higher creaming index of 40 % v/v oil loading. Regardless, no apparent oiling off was noted in all emulsion samples after 14 days of storage signifying excellent Pickering emulsion stability. The droplet size had a generally increasing trend with storage time, and the smallest droplet size was achieved at 10 % v/v. In addition, the Pickering emulsion droplet had uniform size distribution even after 14 days of storage demonstrating minimal particle deformation or emulsion destabilization (Figure S3c) [46,48]. The uniform size distribution of MLP-stabilized Pickering emulsion at different oil loading was also in good agreement with the microscopic images (Fig. 5**c**). Excellent emulsion stability at different oil loading is advantageous as it imparts versatility to the design, allowing the hosting and delivery of hydrophobic drugs in the oil phase and hydrophilic drugs in the aqueous lumen of MLP at different ratios depending on their application [49,50]. Here onwards, Pickering emulsion stabilized by MLP at pH 7.4 and 30 % w/v concentration at 10 % v/v oil loading will be used for the subsequent analysis.

3.4. Storage stability of MLP-stabilized Pickering emulsion

The storage stability of MLP-stabilized Pickering emulsion was evaluated by subjecting freshly formed emulsion at pH 7.4 MLP suspension, 30 % w/v MLP concentration, and 10 % v/v oil loading to 4°C, 25°C, and 45°C environment for 21 days. While apparent creaming was still noticed in the emulsion samples, the droplet size did not significantly change at 4°C and 25°C indicating the stability of phosphatidylcholine-based MLP at lower temperature (Fig. 6**a and b**). At 45°C, an increase in droplet size from 12.3 ± 0.9 μm to 59.0 ± 22.7

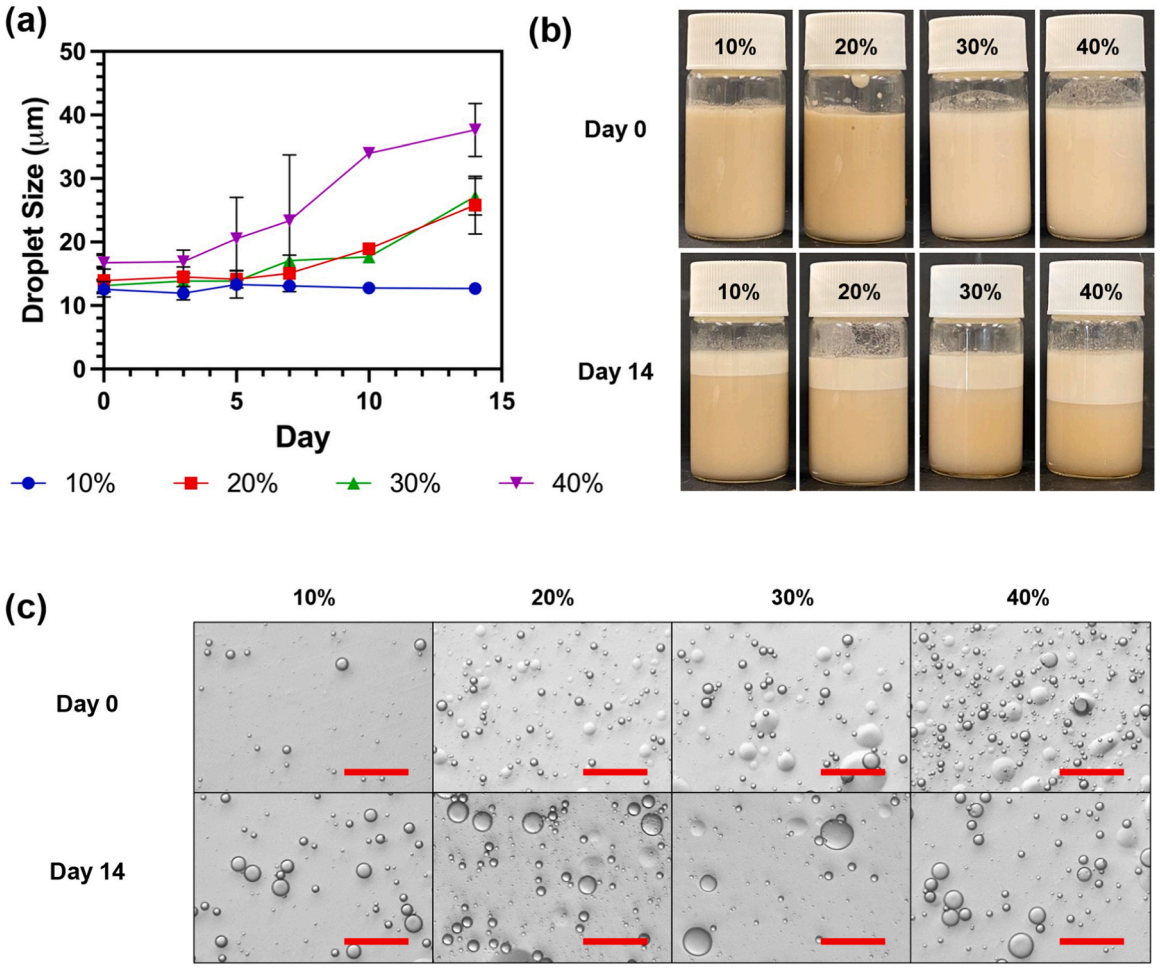

Fig. 5. Effect of oil loading on Pickering emulsion stability. (a) Droplet size, (b) creaming profile, and (c) microscopic images of MLP-stabilized Pickering emulsion at different oil loading from day 0 to day 14. The scale bar is 50 μm. The error bars represent the standard deviation in measurements.

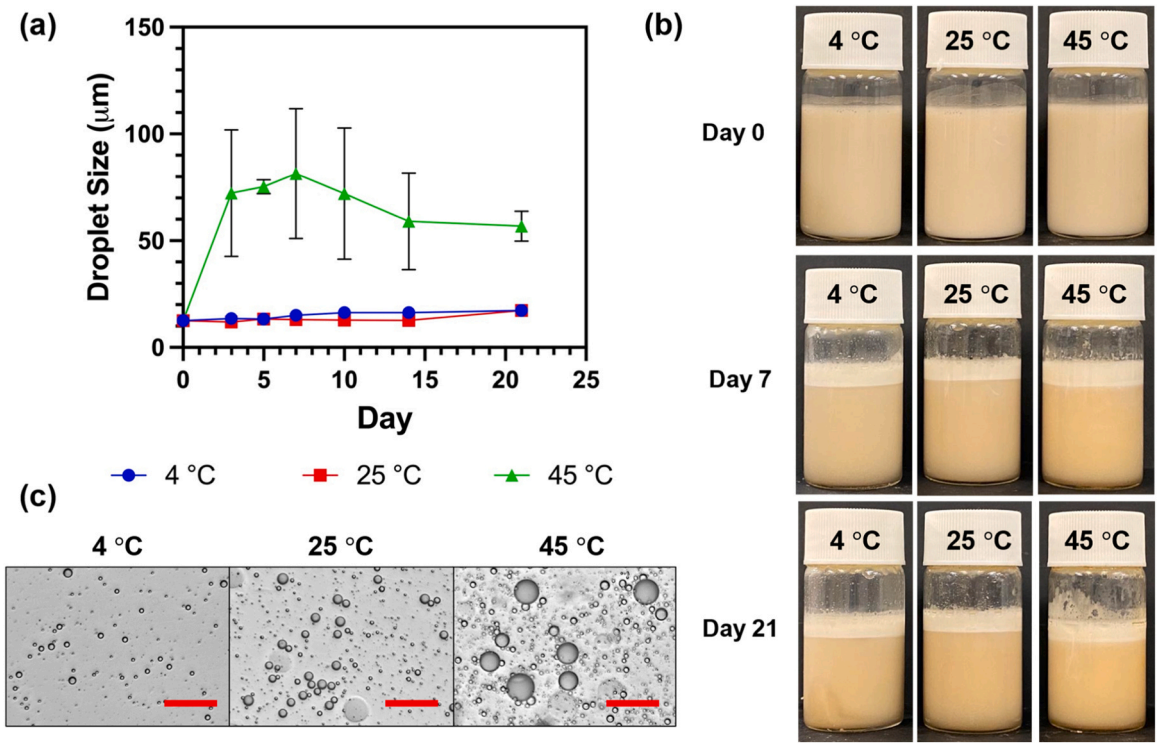

Fig. 6. Storage stability of MLP-stabilized Pickering emulsion. (a) Droplet size, (b) creaming profile, and (c) microscopic images of MLP-stabilized Pickering emulsion at different temperatures from day 0 to day 21. The scale bar is 50 μm. The error bars represent the standard deviation in measurements.

μm after 21 days of storage was observed (Fig. 6**a**). This increase in droplet size could be attributed to the transition of phosphatidylcholine from one phase to another as it surpasses its gel-to-liquid phase transition temperature or T_m (~45°C) (Figure S4). At a temperature above T_m, the MLP is more prone to fusion or aggregation as lipid membranes have increased fluidity and permeability [15]. As the MLP is continuously exposed to a temperature greater than T_m, the structural integrity of the membrane is compromised leading to MLP destabilization [15,18]. Consequently, the repulsion force between emulsion droplets is reduced causing them to coalesce as reflected in the microscopic images (Fig. 6**c**) [18,39].

3.5. pH responsiveness of MLP-stabilized Pickering Emulsion

The pH-responsiveness of the MLP-stabilized Pickering emulsion was investigated by exposing them to pH variation. The freshly formed emulsion was tuned to pH 1.5, 3.0, 5.0, 6.0, and 8.5 by the addition of 1.0 M HCl or 1.0 M NaOH where the droplet size, morphology, and visual appearance were then examined. The results unveiled that the emulsion remained relatively stable at 8.5 with a slight increase in droplet size to 23.2 ± 4.3 μm. As pH decreased to 1.5, severe droplet flocculation was noticed owing to the poor interface coverage by protonated MLP (Fig. 7**a**). Evident phase separation was also noted for emulsion tuned to pH 1.5. To further understand the behavior of MLP-stabilized Pickering emulsion under pH variation, the emulsions at different pH were tuned back to the initial pH. The visual appearance of all emulsions remained similar except for the emulsion at pH 1.5 (Fig. 7**b**). Upon tuning to the initial pH, the emulsion stability was instantaneously restored. Not only did the phase separation disappear but there was a reduction in droplet size. The degree of droplet flocculation was also reduced as a result of phosphate group deprotonation when the pH of the emulsion approached phosphate group pKa. Similar observations and theory for emulsion tuned from pH 3.0, 5.0, and 6.0 to the initial pH apply. Another interesting observation noticed for emulsions tuned from pH 7.4–8.5 was that there was an increase in droplet size which could also be attributed to the reduced surface charge as phosphate groups undergo protonation.

To recapitulate the inherent drug delivery process *via* the gastrointestinal digestion tract, the Pickering emulsion was subjected to sequential pH to study its stability and recoverability as a potential drug delivery vehicle. The stable emulsion formed was sequentially exposed to the stomach (~pH 1.5), intestine (~pH 7.4), and colon (~pH 8.5) environment. Fig. 7**c** showed an increase in droplet size from 12.3 ± 0.9 μm to 95.9 ± 19.9 μm after tuning the emulsion to pH 1.5 where creaming also occurred (Fig. 7**d**). By adjusting the emulsion pH to 7.4, the droplet size was reduced to 38.2 ± 5.4 μm with evidently less droplet flocculation (Fig. 7**e**). Further increasing the pH to 8.5 led to a decrease in droplet size to 31.7 ± 1.3 μm where droplet aggregation considerably diminished. Reduction in droplet size from pH 1.5–8.5 can be associated with the deprotonation of phosphate group. After phosphate group deprotonation, droplets are less prone to flocculate as inter-droplet repulsive energy is restored. No evident deoiling was observed in the cream phase after the sequential pH tuning. To further improve the stability of liposome-based formulation under a gastrointestinal environment, various modifications have been proposed. Among them, coating liposomes with pH-responsive polymers has drawn substantial attention as they preserve liposome functionality and integrity under different pH environments for targeted cargo release [51–54].

3.6. Magnetic responsiveness of MLP-stabilized Pickering emulsion

The magnetic responsiveness of MLP-stabilized Pickering emulsion was investigated by subjecting the emulsion to an external magnetic force. Evidently, the MLP-stabilized Pickering emulsion promptly responded to the external magnetic field (Fig. 8**a**). The outcome of this analysis suggests that the SPION retained its magnetic responsiveness after being encapsulated within the liposome. In this study, it is desirable to incorporate magnetic guiding properties into the Pickering emulsion while ensuring the emulsion stability is not compromised under an external magnetic field. The capability of the emulsion to

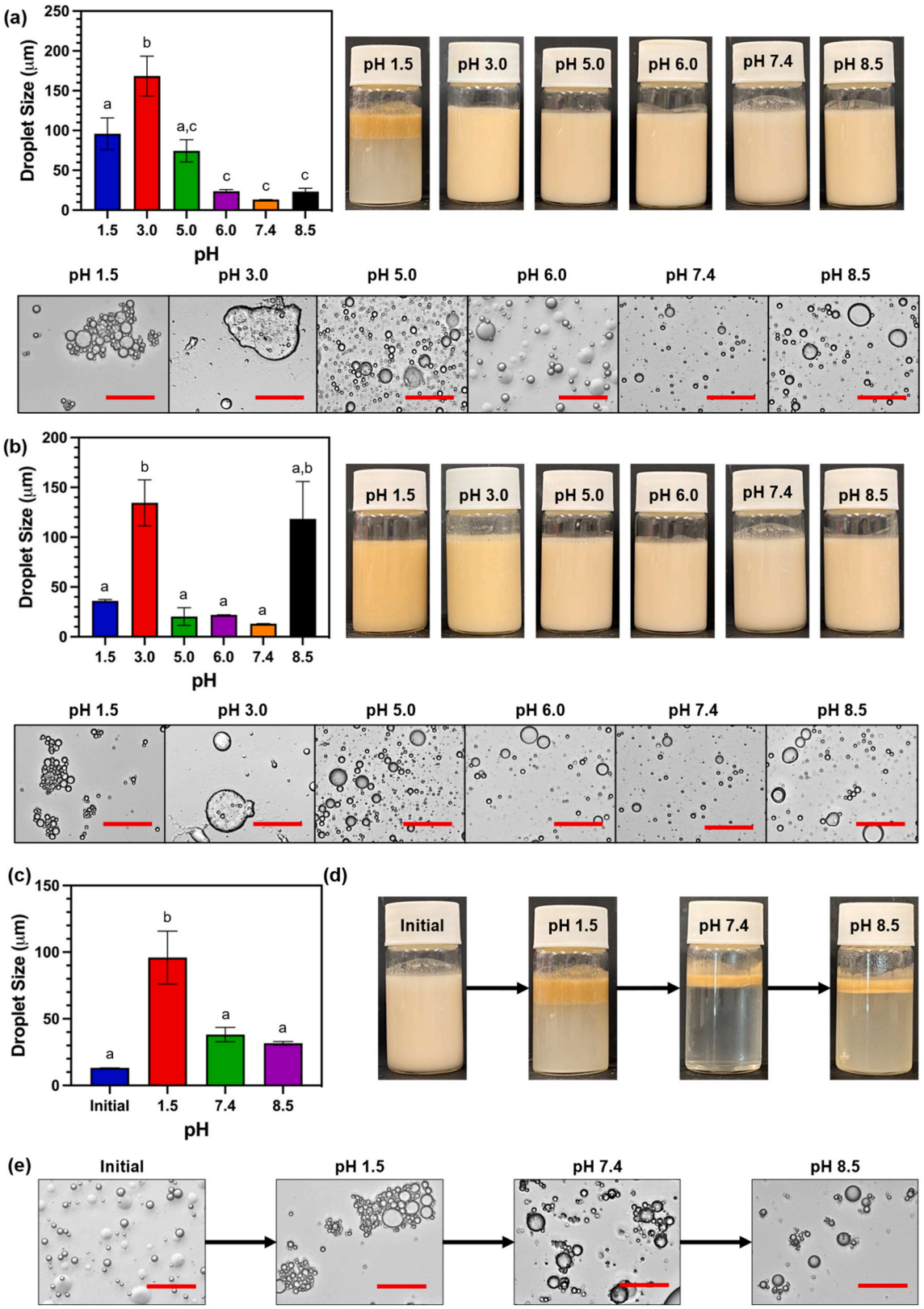

Fig. 7. pH-responsiveness of MLP-stabilized Pickering emulsion. Droplet size, creaming profile, and microscopic images of MLP-stabilized Pickering emulsion (a) tuned from initial pH to pH 1.5, 3.0, 5.0, 6.0, 7.4, and 8.5; (b) tuned from pH 1.5, 3.0, 5.0, 6.0, 7.4 and 8.5 to initial pH. Sequential pH-responsiveness of MLP-stabilized Pickering emulsion. (c) Droplet size, (d) creaming profile, and (e) microscopic images of MLP-stabilized Pickering emulsion when subjected to sequential pH variation. The scale bar is 50 μm. The error bars represent the standard deviation in measurements and different alphabetic letters were significantly different at $p \leq 0.05$ by Bonferroni's Multiple Comparison Test.

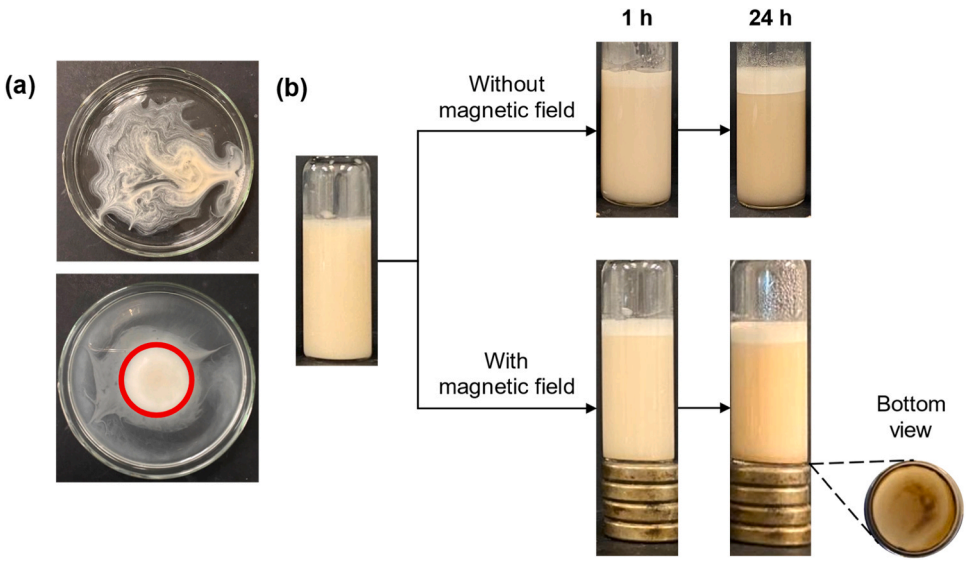

Fig. 8. Magnetic responsiveness of MLP-stabilized Pickering emulsion. (a) Magnetic-responsiveness of MLP-stabilized Pickering emulsion (red circle represents the location of magnet). (b) Stability study of MLP-stabilized Pickering emulsion with and without magnetic field at 0 h, 1 h, and 24 h.

withstand demulsification was investigated by placing a neodymium magnet at the bottom of the emulsion vial for an extended period (Fig. 8**b**). The demulsification process was monitored by photographing the vials at 0 h, 1 h, and 24 h. In the case of demulsification, clear oil and aqueous MLP suspension phase separation will be observed [27–30]. No phase separation was observed, but a similar creaming profile was noticed in Pickering emulsion samples with or without a magnetic field. It was also observed that there was SPION sedimentation at the bottom of the vial after exposing it to a magnetic field for 24 h. The release of SPION from the liposome through mechanical distortion of the membrane was previously reported to potentially damage the membrane integrity [55]. Given the small size of SPION used in this study (8.8 ± 1.2 nm), liposome membranes are less prone to mechanical distortion after SPION release [56,57]. Additionally, MLP membrane assembly using unsaturated lipids - phosphatidylcholine and cholesterol exhibits the capacity to regain structural integrity post-SPION release under a moderate magnetic field [58,59]. In this regard, the liposome retained its structural integrity as a Pickering emulsifier even after the SPION release preventing emulsion destabilization.

4. Conclusion

In this work, we successfully developed a dual pH and magnetic-responsive Pickering emulsion stabilized by MLP. The pH of MLP suspension, MLP concentration, and oil loading can individually affect the Pickering emulsion stability. Among different formulations, stable Pickering emulsion was formed at MLP pH 7.4, 30 % MLP concentration, and 10 % v/v oil loading. Besides, the MLP-stabilized Pickering emulsion was found to remain stable for up to 21 days when stored at a temperature lower than the T_m of MLP. The Pickering emulsion also exhibited both pH and magnetic responsiveness. MLP-stabilized Pickering emulsion demonstrated excellent stability when subjected to alkali pH due to MLP deprotonation. When subjected to sequential pH variation to replicate the gastrointestinal digestion tract, emulsion stability was recovered. This study also unveiled the remarkable magnetic responsiveness of the Pickering emulsion under an external field without demulsification. This discovery holds significance as it simultaneously facilitates the magnetic guidance of Pickering emulsion as a drug delivery vehicle to a specific site while preventing premature cargo release. All in all, this study instigates a new approach in the development of dual pH and magnetic responsive Pickering emulsion, serving as a potential drug delivery vehicle with the ability to co-encapsulate hydrophobic and hydrophilic drugs.

CRediT authorship contribution statement

Chin Siew Sia: Conceptualization, Methodology, Investigation, Validation, Writing – original draft, Writing – review & editing, Visualization. **Beng Ti Tey**: Supervision, Writing – review & editing. **Bey-Hing Goh**: Writing – review & editing. **Liang Ee Low**: Conceptualization, Supervision, Writing – review & editing, Validation, Funding acquisition.

Declaration of Competing Interest

The authors declare that they have no known competing financial interests or personal relationships that could have appeared to influence the work reported in this paper.

Data availability

Data will be made available on request.

Acknowledgment

This work was supported by the Seed Grant from Monash University Malaysia: I-M010-SED-000142.

This work was supported by Geran Penyelidikan Negeri Selangor (GPNS) 2023, Malaysia (SUK/GPNS/2023/PEM/03).

We would like to extend our acknowledgement to Professor Ong Boon Hoong from Nanotechnology and Catalysis Research Centre, University of Malaya for the help in conducting VSM analysis.

Appendix A. Supporting information

Supplementary data associated with this article can be found in the online version at doi:10.1016/j.colsurfb.2024.114051.

References

[1] Z. Sun, X. Yan, Y. Xiao, L. Hu, M. Eggersdorfer, D. Chen, Z. Yang, D.A. Weitz, Pickering emulsions stabilized by colloidal surfactants: Role of solid particles, Particuology 64 (2022) 153–163.

[2] T. Xia, C. Xue, Z. Wei, Physicochemical characteristics, applications and research trends of edible Pickering emulsions, Trends Food Sci. Technol. 107 (2021) 1–15.

[3] S.K. Wong, L.E. Low, J. Supramaniam, S. Manickam, T.W. Wong, C.H. Pang, S. Y. Tang, Physical stability and rheological behavior of Pickering emulsions stabilized by protein–polysaccharide hybrid nanoconjugates, Nanotechnol. Rev. 10 (2021) 1293–1305.
[4] S.K. Wong, M.I.A. Mohd Ali, L.E. Low, J. Supramaniam, S. Manickam, T.W. Wong, G. Garnier, S.Y. Tang, Transforming the Chemical Functionality of Nanocellulose for Applications in Food Pickering Emulsions: A Critical Review, Food Reviews International, 2023, pp. 1–25.
[5] K.W. Ho, C.W. Ooi, W.W. Mwangi, W.F. Leong, B.T. Tey, E.-S. Chan, Comparison of self-aggregated chitosan particles prepared with and without ultrasonication pretreatment as Pickering emulsifier, Food Hydrocoll. 52 (2016) 827–837.
[6] W.W. Mwangi, K.-W. Ho, B.-T. Tey, E.-S. Chan, Effects of environmental factors on the physical stability of pickering-emulsions stabilized by chitosan particles, Food Hydrocoll. 60 (2016) 543–550.
[7] Z. Hu, S. Ballinger, R. Pelton, E.D. Cranston, Surfactant-enhanced cellulose nanocrystal Pickering emulsions, J. Colloid Interface Sci. 439 (2015) 139–148.
[8] Z. Zhang, Z. Zhang, T. Chang, J. Wang, X. Wang, G. Zhou, Phase change material microcapsules with melamine resin shell via cellulose nanocrystal stabilized Pickering emulsion in-situ polymerization, Chem. Eng. J. 428 (2022) 131164.
[9] L.E. Low, B.T. Tey, B.H. Ong, E.S. Chan, S.Y. Tang, Palm olein-in-water Pickering emulsion stabilized by Fe3O4-cellulose nanocrystal nanocomposites and their responses to pH, Carbohydr. Polym. 155 (2017) 391–399.
[10] C.S. Sia, H.P. Lim, Y.N. Lin, L.C. Beh, B.T. Tey, B.-H. Goh, L.E. Low, pH-controllable stability of iron oxide@chitosan nanocomposite-stabilized magnetic Pickering emulsions, Eur. Polym. J. 186 (2023) 111870.
[11] A. Mukherjee, B. Bisht, S. Dutta, M.K. Paul, Current advances in the use of exosomes, liposomes, and bioengineered hybrid nanovesicles in cancer detection and therapy, Acta Pharmacol. Sin. 43 (2022) 2759–2776.
[12] S. Wang, Y. Chen, J. Guo, Q. Huang, Liposomes for Tumor Targeted Therapy: A Review, Int. J. Mol. Sci. (2023).
[13] M.I. Priester, T.L.M. ten Hagen, Image-guided drug delivery in nanosystem-based cancer therapies, Adv. Drug Deliv. Rev. 192 (2023) 114621.
[14] C.G.A. Das, V.G. Kumar, T.S. Dhas, V. Karthick, C.M.V. Kumar, Nanomaterials in anticancer applications and their mechanism of action - A review, Nanomed.: Nanotechnol., Biol. Med. 47 (2023) 102613.
[15] D.E. Large, R.G. Abdelmessih, E.A. Fink, D.T. Auguste, Liposome composition in drug delivery design, synthesis, characterization, and clinical application, Adv. Drug Deliv. Rev. 176 (2021) 113851.
[16] Y. Lee, D.H. Thompson, Stimuli-responsive liposomes for drug delivery, WIREs Nanomed. Nanobiotechnology 9 (2017) e1450.
[17] C.S. Sia, H.P. Lim, B.T. Tey, B.-H. Goh, L.E. Low, Stimuli-responsive nanoassemblies for targeted delivery against tumor and its microenvironment, Biochim. Et. Biophys. Acta (BBA) - Rev. Cancer 1877 (2022) 188779.
[18] Y. Sun, W. Tang, C. Pu, R. Li, Q. Sun, H. Wang, Improved stability of liposome-stabilized emulsions as a co-encapsulation delivery system for vitamin B2, vitamin E and β-carotene, Food Funct. 13 (2022) 2966–2984.
[19] W. Liu, J. Liu, L.J. Salt, M.J. Ridout, J. Han, P.J. Wilde, Structural stability of liposome-stabilized oil-in-water pickering emulsions and their fate during in vitro digestion, Food Funct. 10 (2019) 7262–7274.
[20] L.E. Low, H.P. Lim, Y.S. Ong, S.P. Siva, C.S. Sia, B.-H. Goh, E.S. Chan, B.T. Tey, Stimuli-controllable iron oxide nanoparticle assemblies: Design, manipulation and bio-applications, J. Control. Release 345 (2022) 231–274.
[21] L.E. Low, J. Wu, J. Lee, B.T. Tey, B.-H. Goh, J. Gao, F. Li, D. Ling, Tumor-responsive dynamic nanoassemblies for targeted imaging, therapy and microenvironment manipulation, J. Control. Release 324 (2020) 69–103.
[22] V. De Leo, A.M. Maurelli, L. Giotta, L. Catucci, Liposomes containing nanoparticles: preparation and applications, Colloids Surf. B: Biointerfaces 218 (2022) 112737.
[23] Z. Zhuo, J. Wang, Y. Luo, R. Zeng, C. Zhang, W. Zhou, K. Guo, H. Wu, W. Sha, H. Chen, Targeted extracellular vesicle delivery systems employing superparamagnetic iron oxide nanoparticles, Acta Biomater. 134 (2021) 13–31.
[24] M. Pourmadadi, M. Ahmadi, F. Yazdian, Synthesis of a novel pH-responsive Fe3O4/chitosan/agarose double nanoemulsion as a promising Nanocarrier with sustained release of curcumin to treat MCF-7 cell line, Int. J. Biol. Macromol. 235 (2023) 123786.
[25] L.E. Low, L.T.-H. Tan, B.-H. Goh, B.T. Tey, B.H. Ong, S.Y. Tang, Magnetic cellulose nanocrystal stabilized Pickering emulsions for enhanced bioactive release and human colon cancer therapy, Int. J. Biol. Macromol. 127 (2019) 76–84.
[26] W.W. Mwangi, H.P. Lim, L.E. Low, B.T. Tey, E.S. Chan, Food-grade Pickering emulsions for encapsulation and delivery of bioactives, Trends Food Sci. Technol. 100 (2020) 320–332.
[27] T. Lü, S. Zhou, R. Ma, D. Qi, Y. Sun, D. Zhang, J. Huang, H. Zhao, Demulsification Performance and Mechanism of Tertiary Amine Polymer-Grafted Magnetic Nanoparticles in Surfactant-Free Oil-in-Water Emulsion, Langmuir 39 (2023) 1288–1298.
[28] Q. Wang, M.C. Puerto, S. Warudkar, J. Buehler, S.L. Biswal, Recyclable amine-functionalized magnetic nanoparticles for efficient demulsification of crude oil-in-water emulsions, Environ. Sci.: Water Res. Technol. 4 (2018) 1553–1563.
[29] H. Yang, Q. Hou, S. Wang, D. Guo, G. Hu, Y. Xu, J. Tai, X. Wu, D. Yu, J. Wang, Magnetic-responsive switchable emulsions based on Fe3O4@SiO2–NH2 nanoparticles, Chem. Commun. 54 (2018) 10679–10682.
[30] H. Yang, S. Wang, W. Zhang, J. Wu, S. Yang, D. Yu, X. Wu, Y. Sun, J. Wang, Rapid demulsification of pickering emulsions triggered by controllable magnetic field, Sci. Rep. 10 (2020) 16565.
[31] T. Hyeon, S.S. Lee, J. Park, Y. Chung, H.B. Na, Synthesis of Highly Crystalline and Monodisperse Maghemite Nanocrystallites without a Size-Selection Process, J. Am. Chem. Soc. 123 (2001) 12798–12801.
[32] K. Ulbrich, K. Holá, V. Šubr, A. Bakandritsos, J. Tuček, R. Zbořil, Targeted Drug Delivery with Polymers and Magnetic Nanoparticles: Covalent and Noncovalent Approaches, Release Control, Clin. Stud., Chem. Rev. 116 (2016) 5338–5431.
[33] V.F. Cardoso, A. Francesko, C. Ribeiro, M. Bañobre-López, P. Martins, S. Lanceros-Mendez, Advances in Magnetic Nanoparticles for Biomedical Applications, Adv. Healthc. Mater. 7 (2018) 1700845.
[34] Z. Al-Ahmady, N. Lozano, K.-C. Mei, W.T. Al-Jamal, K. Kostarelos, Engineering thermosensitive liposome-nanoparticle hybrids loaded with doxorubicin for heat-triggered drug release, Int. J. Pharm. 514 (2016) 133–141.
[35] A. Askari, S. Tajvar, M. Nikkhah, S. Mohammadi, S. Hosseinkhani, Synthesis, characterization and in vitro toxicity evaluation of doxorubicin-loaded magnetoliposomes on MCF-7 breast cancer cell line, J. Drug Deliv. Sci. Technol. 55 (2020) 101447.
[36] C. Bonnaud, C.A. Monnier, D. Demurtas, C. Jud, D. Vanhecke, X. Montet, R. Hovius, M. Lattuada, B. Rothen-Rutishauser, A. Petri-Fink, Insertion of Nanoparticle Clusters into Vesicle Bilayers, ACS Nano 8 (2014) 3451–3460.
[37] B. Chen, R. Zhang, H. Wu, M. Li, G. Zhou, M. Ji, Thermoresponsive magnetoliposome encapsulating doxorubicin and high performance Ferumoxytol for effective tumor synergistic therapy in vitro, J. Drug Deliv. Sci. Technol. 57 (2020) 101677.
[38] B. Clares, R.A. Biedma-Ortiz, E. Sáez-Fernández, J.C. Prados, C. Melguizo, L. Cabeza, R. Ortiz, J.L. Arias, Nano-engineering of 5-fluorouracil-loaded magnetoliposomes for combined hyperthermia and chemotherapy against colon cancer, Eur. J. Pharm. Biopharm. 85 (2013) 329–338.
[39] L.E. Low, S.P. Siva, Y.K. Ho, E.S. Chan, B.T. Tey, Recent advances of characterization techniques for the formation, physical properties and stability of Pickering emulsion, Adv. Colloid Interface Sci. 277 (2020) 102117.
[40] J. Xiao, Y. Li, Q. Huang, Recent advances on food-grade particles stabilized Pickering emulsions: Fabrication, characterization and research trends, Trends Food Sci. Technol. 55 (2016) 48–60.
[41] M. Wojciechowski, T. Grycuk, J.M. Antosiewicz, B. Lesyng, Prediction of Secondary Ionization of the Phosphate Group in Phosphotyrosine Peptides, Biophys. J. 84 (2003) 750–756.
[42] P. Bhatt, X. Zhou, Y. Huang, W. Zhang, S. Chen, Characterization of the role of esterases in the biodegradation of organophosphate, carbamate, and pyrethroid pesticides, J. Hazard. Mater. 411 (2021) 125026.
[43] F. Degli-Innocenti, T. Breton, S. Chinaglia, E. Esposito, M. Pecchiari, A. Pennacchio, A. Pischedda, M. Tosin, Microorganisms that produce enzymes active on biodegradable polyesters are ubiquitous, Biodegradation 34 (2023) 489–518.
[44] S. Barekat, A. Nasirpour, J. Keramat, M. Dinari, M. Claeys, A. Sedaghat Doost, P. Van der Meeren, Formulation, characterization, and physical stability of encapsulated walnut green husk (Juglans regia L.) extract in phosphatidylcholine liposomes, Journal of Dispersion Science and Technology, 1-14.
[45] B.P. Binks, S.O. Lumsdon, Pickering Emulsions Stabilized by Monodisperse Latex Particles: Effects of Particle Size, Langmuir 17 (2001) 4540–4547.
[46] J. Wu, G.-H. Ma, Recent Studies of Pickering Emulsions: Particles Make the Difference, Small 12 (2016) 4633–4648.
[47] F. Zhu, Starch based Pickering emulsions: Fabrication, properties, and applications, Trends Food Sci. Technol. 85 (2019) 129–137.
[48] C. Albert, M. Beladjine, N. Tsapis, E. Fattal, F. Agnely, N. Huang, Pickering emulsions: Preparation processes, key parameters governing their properties and potential for pharmaceutical applications, J. Control. Release 309 (2019) 302–332.
[49] H. Chen, H. Dai, H. Zhu, L. Ma, Y. Fu, X. Feng, Y. Sun, Y. Zhang, Construction of dual-compartmental micro-droplet via shrimp ferritin nanocages stabilized Pickering emulsions for co-encapsulation of hydrophobic/hydrophilic bioactive compounds, Food Hydrocoll. 126 (2022) 107443.
[50] C. Setti, G. Suarato, G. Perotto, A. Athanassiou, I.S. Bayer, Investigation of in vitro hydrophilic and hydrophobic dual drug release from polymeric films produced by sodium alginate-MaterBi® drying emulsions, Eur. J. Pharm. Biopharm. 130 (2018) 71–82.
[51] H. Alghurabi, T. Tagami, K. Ogawa, T. Ozeki, Preparation, Characterization and In Vitro Evaluation of Eudragit S100-Coated Bile Salt-Containing Liposomes for Oral Colonic Delivery of Budesonide, Polymers (2022).
[52] M.J. Barea, M.J. Jenkins, M.H. Gaber, R.H. Bridson, Evaluation of liposomes coated with a pH responsive polymer, Int. J. Pharm. 402 (2010) 89–94.
[53] E. Yang, H.-S. Jung, P.-S. Chang, Stimuli-responsive polymer-complexed liposome nanocarrier provides controlled release of biomolecules, Food Hydrocoll. 125 (2022) 107397.
[54] J. Zhang, C.-Z. Ye, Z.-Y. Liu, Q. Yang, Y. Ye, Preparation And Antibacterial Effects Of Carboxymethyl Chitosan-Modified Photo-Responsive Camellia Sapogenin Derivative Cationic Liposomes, Int. J. Nanomed. 14 (2019) 8611–8626.
[55] B. Shirmardi Shaghasemi, M.M. Virk, E. Reimhult, Optimization of Magneto-thermally Controlled Release Kinetics by Tuning of Magnetoliposome Composition and Structure, Sci. Rep. 7 (2017) 7474.
[56] K.M. Krishnan, Biomedical Nanomagnetics: A Spin Through Possibilities in Imaging, Diagnostics, and Therapy.

[57] E. Amstad, J. Kohlbrecher, E. Müller, T. Schweizer, M. Textor, E. Reimhult, Triggered Release from Liposomes through Magnetic Actuation of Iron Oxide Nanoparticle Containing Membranes, Nano Lett. 11 (2011) 1664–1670.
[58] K.Y. Vlasova, A. Piroyan, I.M. Le-Deygen, H.M. Vishwasrao, J.D. Ramsey, N. L. Klyachko, Y.I. Golovin, P.G. Rudakovskaya, I.I. Kireev, A.V. Kabanov, M. Sokolsky-Papkov, Magnetic liposome design for drug release systems responsive to super-low frequency alternating current magnetic field (AC MF), J. Colloid Interface Sci. 552 (2019) 689–700.
[59] C. Loudet, A. Diller, A. Grélard, R. Oda, E.J. Dufourc, Biphenyl phosphatidylcholine: A promoter of liposome deformation and bicelle collective orientation by magnetic fields, Prog. Lipid Res. 49 (2010) 289–297.